TISSUE ENGINEERING: Part A
Volume 17, Numbers 1 and 2, 2011

DOI: 10.1089/ten.tea.2009.0807

Investigation of the Regenerative Capacity of an Acellular Porcine Medial Meniscus for Tissue Engineering Applications

Thomas W. Stapleton, Ph.D.,[1] Joanne Ingram, Ph.D.,[1] John Fisher, Ph.D.,[2] and Eileen Ingham, Ph.D.[1]

Previously, we have described the development of an acellular porcine meniscal scaffold. The aims of this study were to determine the immunocompatibility of the scaffold and capacity for cellular attachment and infiltration to gain insight into its potential for meniscal repair and replacement. Porcine menisci were decellularized by exposing the tissue to freeze–thaw cycles, incubation in hypotonic tris buffer, 0.1% (w/v) sodium dodecyl sulfate in hypotonic buffer plus protease inhibitors, nucleases, hypertonic buffer followed by disinfection using 0.1% (v/v) peracetic, and final washing in phosphate-buffered saline. *In vivo* immunocompatibility was assessed after implantation of the acellular meniscal scaffold subcutaneously into galactosyltransferase knockout mice for 3 months in comparison to fresh and acellular tissue treated with α-galactosidase (negative control). The cellular infiltrates in the explants were assessed by histology and characterized using monoclonal antibodies against: CD3, CD4, CD34, F4/80, and C3c. Static culture was used to assess the potential of acellular porcine meniscal scaffold to support the attachment and infiltration of primary human dermal fibroblasts and primary porcine meniscal cells *in vitro*. The explants were surrounded by capsules that were more pronounced for the fresh meniscal tissue compared to the acellular tissues. Cellular infiltrates compromised mononuclear phagocytes, CD34-positive cells, and nonlabeled fibroblastic cells. T-lymphocytes were sparse in all explanted tissue types and there was no evidence of C3c deposition. The analysis revealed an absence of a specific immune response to all of the implanted tissues. Acellular porcine meniscus was shown to be capable of supporting the attachment and infiltration of primary human fibroblasts and primary porcine meniscal cells. In conclusion, acellular porcine meniscal tissue exhibits excellent immunocompatibility and potential for cellular regeneration in the longer term.

Introduction

The menisci of the knee are predominantly fibrocartilage in nature with a specialized arrangement of collagen fibers and hyaline-like cartilage providing structural integrity when in tension and compression. The structural organization highlights two major roles of the meniscus: (1) stress distribution and (2) load transmission. The dual role of this tissue within the knee joint is critical for efficient and nonproblematic joint functioning.

Injuries resulting in tears represent the major mechanism by which meniscal function is compromised. Tears may take multiple paths through the meniscal body, dictating the likelihood of healing. Vertical tears that run parallel with the circumferential collagen fibers may heal completely, especially when in communication with the vascular periphery.[1,2] In contrast, tears that disrupt the collagen structure often lead to loss of load transmission resulting in meniscal failure.[2]

With an ever increasing number of injuries sustained to menisci, there is a growing need to develop a successful repair treatment or replacement meniscal tissue. Where injuries are irreparable, surgeons have traditionally removed the damaged region of the meniscus through partial or complete meniscectomy. Loss of meniscal tissue has, however, been directly correlated to changes in contact stresses in the knee joint resulting in the development of osteoarthritis of the articular cartilage.[3–5]

When repair is not possible, replacement of the meniscus is now the option of choice. Currently, meniscus allografts represent the gold standard for meniscal replacement. However, limitations of meniscal allografts, including availability, sizing, and disease transmission, accentuate the need for alternatives.[6,7] Replacement of the meniscus with artificial implants still requires substantial experimental evaluation with a recent preclinical study failing to demonstrate evidence of chondroprotection.[8]

[1]Institute of Molecular and Cellular Biology, The University of Leeds, Leeds, United Kingdom.
[2]School of Mechanical Engineering, The University of Leeds, Leeds, United Kingdom.

Most recently, several groups have taken tissue engineering approaches to develop a replacement meniscus, with the majority investigating the use of natural scaffolds with or without a cellular component.[9–17] In the case of the cellular constructs, it is hypothesized that once implanted into the defect, cells of donor origin will survive and maintain the matrix until recipient cells infiltrate and regenerate the tissue.[18] In the case of the acellular implant, it is hypothesized that the recipients' endogenous cells will be encouraged to infiltrate from the surrounding tissue and serve to regenerate the scaffold. Both approaches have advantages and disadvantages and it will be important to determine which offers the optimal approach for meniscal replacement through extensive preclinical studies. We have previously developed an acellular porcine meniscus scaffold that is biocompatible and retains the collagenous architecture and biomechanical properties of the natural tissue.[14] This acellular meniscus scaffold provides a platform technology for investigating *in vitro* and *in vivo* regenerative approaches.

The aims of this study were to investigate the immunocompatibility of the acellular porcine meniscal tissue and its potential for cellular repopulation. The objectives were (1) to investigate the host response to the scaffold in galactosyltransferase knockout (GTKO) mice and (2) determine the capacity of meniscal cells and fibroblasts to attach to and infiltrate the acellular scaffold *in vitro*.

Materials and Methods

Tissue procurement

Porcine medial menisci were obtained from the local abattoir (J. Penny, Leeds, United Kingdom) within 24 h of animal slaughter. The menisci were dissected from the knee joint by gently excising the knee capsule before cutting both the anterior and posterior cruciate ligaments to expose the meniscus. Incisions were then made perpendicular to the meniscal horn attachments to release the menisci. Excess tissue from the capsule and the meniscal attachments was then removed using scissors. The meniscus was washed in phosphate-buffered saline (PBS; Oxoid) to remove excess blood. Samples were then stored at −40°C on PBS moistened filter paper.

Decellularization

Decellularization was performed as described previously.[14] Meniscal samples were subjected to three cycles of dry freeze–thaw by freezing the samples at −20°C for 3 h before leaving the tissue to thaw at room temperature for 4 h. This was followed by subjecting the tissue to three more cycles of freeze–thaw in hypotonic (10 mM tris-HCl, pH 8.0; Sigma) buffer. Samples were then cycled through hypotonic buffer at 4°C for 24 h, hypotonic buffer at 37°C for 24 h, followed by incubation in anionic-detergent (0.1% [w/v] sodium dodecyl sulfate; Sigma) at 45°C for 48 h, three times with agitation in the presence of protease inhibitors (aprotinin, 10 KIU.mL^{-1}; Trasylol; Bayer and 0.1% [w/v] ethylene diamine tetraacetic acid; VWR). Samples were washed in PBS with aprotinin three times for 12 h with agitation. After washing, samples were incubated three times in DNase (50 U·mL^{-1}; Sigma) and RNase (1 U·mL^{-1}; Sigma) in buffer (50 mM tris-HCl, 10 mM $MgCl_2$, 50 μg·mL^{-1} bovine serum albumin [BSA; Sigma] at pH 7.5) for 3 h at 37°C with gentle agitation. Tissue was then washed in hypertonic buffer (1.5 M NaCl in 0.05 M tris-HCl, pH 7.6) before washing in PBS with protease inhibitors for 24 h at room temperature. A decontamination step, consisting of incubating samples in 0.1% (v/v) peracetic acid (PAA; Sigma) in PBS for 3 h was then incorporated to achieve surface disinfection of the tissue samples.[19] Finally, meniscal samples were washed five times in PBS at 45°C, 37°C, and 4°C, respectively, for 24 h.

α-Galactosidase treatment

Acellular menisci were chopped into 3 mm^3 samples and treated with α-galactosidase (1 U·mL^{-1} [Sigma] in 0.05 M tris-HCl pH 6; 1 mL per 100 mg tissue) for 24 h at 37°C while being rotated (13 rpm) on a rotator.

In vivo *immunocompatibility study*

The host response to fresh ($n = 4$), decellularized ($n = 6$) and α-galactosidase treated ($n = 4$) porcine medial meniscal tissue was assessed in a mouse subcutaneous implant model using female GTKO mice (BresaGen Xenograft Management, Ltd.) that had (human-like model) and had not been immunized with porcine red blood cells. Fresh porcine medial meniscal samples were left untreated. α-Galactosidase-treated tissue was used as a negative control. Two tissue samples per mouse were implanted for both the immunized and nonimmunized groups.

Immunization was performed by injecting 0.2 mL of packed porcine red blood cells into the peritoneum of the mice at days 0 and 14. Tissue was implanted on day 28 under short-term anesthesia. The mid-dorsum of the mice was aseptically prepared using 70% (v/v) ethanol. Tissue samples (3 mm^3) from the central meniscal midsubstance were implanted subcutaneously along the middorsal line distant from the skin incision. Mice were fed food and water *ab libitum* and left for a period of 3 months. Mice were then sacrificed by schedule (1) and bled via cardiac puncture, and the implanted tissues retrieved for analysis. All animal procedures were carried out by under appropriate UK Home Office licenses.

Histological assessment of explants and surrounding capsule

Explanted tissue (vaccinated: fresh, $n = 4$, decellularized, $n = 4$, α-galactosidase, $n = 3$; nonvaccinated: fresh, $n = 4$, decellularized, $n = 4$, α-galactosidase, $n = 3$) was divided into two equal samples and cryoembedded (Fig. 1i). One sample was serially sectioned at 6 μm thickness. Two sections were chosen, located at the periphery and center of the original sample (A & C respectively Fig. 1ii). A third section was taken between the peripheral and central locations (B in Fig. 1ii). Hematoxylin and eosin (H&E; Bios Europe Ltd.) staining was used to determine cell infiltration and morphology. Thickness of the capsule surrounding the explanted meniscal tissue was determined by taking six measurements (Image Pro Plus® imaging software; Media Cybernetics) at random locations along the circumference of the tissue explants (A in Fig. 1iii).

Immunohistochemical assessment of cellular phenotype within the implant

The remaining explant sample for all groups (vaccinated: fresh, $n = 4$, decellularized, $n = 4$, α-galactosidase, $n = 3$;

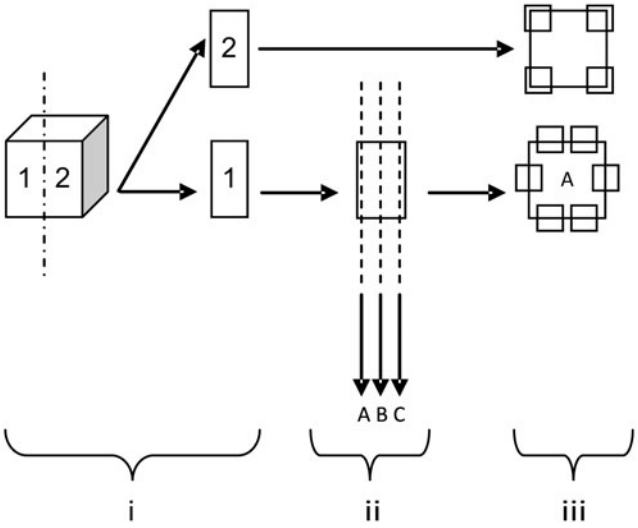

FIG. 1. Diagrammatic overview of sectioning/observation of mouse explants for histological assessment.

nonvaccinated: fresh, $n=4$, decellularized, $n=4$, α-galactosidase, $n=3$) were cryosectioned at 6 μm ("2" in Fig. 1i). Immunolabeling was carried out using an indirect streptavidin-horseradish peroxidase (HRP) immunoperoxidase method at room temperature. Rat monoclonal antibodies to mouse CD3 (pan-mature T-cell; Invitrogen), mouse CD4 (helper T-cell; Invitrogen), mouse CD34 (endothelial cell; BD Biosciences), mouse F4/80 (macrophage; Invitrogen), and mouse C3c (complement; Hycult Biotech) were used to characterize the host response to the tissues. Tris-buffered saline (TBS) was used throughout as diluent and wash buffer. Nonspecific background staining was prevented by blocking with 10% (v/v) rabbit serum (Dako). Sections were first incubated with primary antibody for 1 h, biotinylated rabbit anti-rat secondary antibody (Dako) for 30 min, and streptavidin-HRP complex (R.T.U. HRP Kit; Vector Laboratories) for 45 min with washing between each step. The secondary antibody was absorbed with porcine heart valve tissue to prevent nonspecific background staining. This consisted of finely mincing one valve leaflet and adding it to the antibody diluted 1:5 with antibody diluent (TBS, 0.01% [w/v] sodium azide, 0.1% [w/v] BSA) for 24 h at 4°C while being rotated. After this point, samples were centrifuged at 200 *g* for 10 min before removing the supernatant. This process was repeated a further two times, adding a fresh leaflet to the supernatant each time. Bound antibody was then observed using Sigma Fast 3,3′-diaminobenzidine (Sigma) tablets. Omission of the primary antibody served as a negative control. Positive control tissues (mouse spleen: CD3, CD4, CD34, F4/80; mouse kidney: C3c) and rat anti-mouse isotype control antibodies (IgG1, IgG2a, and IgG2b; Serotec) were used to verify antibody specificity. After labeling, 40× magnification images were captured to provide an overview. Images of 200× magnification were then taken at four preassigned locations on the implant (Fig. 1iii). Each image was analyzed blind and the number of positive cells within each defined area determined.

Enzyme-linked immunosorbent assay for determination of anti-α-gal antibodies in GTKO mouse serum

Immediately after sacrifice of the mice, 500–800 μL of blood was removed by cardiac puncture (vaccinated, $n=6$ [fresh 2, decellularized = 3, α-galactosidase = 1]; nonvaccinated, $n=5$ [fresh = 1, decellularized = 2, α-galactosidase = 2]). The serum was separated after 24 h at 37°C. Serum from normal (Balb/c female) mice was used as a control.

Fifty microliters of α-gal-BSA (10 μg·mL^{-1}; Alexis Biochemicals) was added to the wells of Nunc Maxisorp™ microtiter plates and left overnight at 4°C. The wells were then washed with 300 μL wash buffer (0.05% [v/v] Tween 20 in PBS), three times for 10 min each. Plates were then blocked with 250 μL of 5% (w/v) dried milk protein (Marvel; Morrison's Supermarket) in PBS, for 12 h at 4°C.

Test and control sera were diluted (neat, 1:10, 1:20, 1:40, 1:80, 1:160, 1:320, 1:640, 1:1280, 1:2560, 1:5120, and 1:10,240) with antibody diluent (TBS, 0.01% [w/v] sodium azide, 0.1% [w/v] BSA). The plate wells were then washed with wash buffer, three times for 10 min each before the serum dilutions (100 μL) were added to the α-gal-BSA-coated wells and incubated for 3 h at room temperature. After this, the wells were washed as before and 50 μL secondary rabbit anti-mouse HRP antibody (1:1000; Dako) was added. The plates were then left for 1 h at room temperature. The plates were again washed with wash buffer before adding 100 μL o-phenylenediamine dihydrochloride (OPD) solution (Sigma) and incubating for 10 min at room temperature in the dark. Fifty microliters of 3 M sulfuric acid was added to stop the reaction before the absorbance was read at 492–630 nm. The antibody titers of the test sera were taken as the reciprocal value of the last dilution with an absorbance value greater than or equal to three standard deviations of the normal mouse serum control at the same dilution.

Isolation of meniscal cells from porcine medial menisci

Female, 35 kg large white pigs were sacrificed before aseptic dissection of the medial menisci. The tissue was then incubated (5% CO_2 [v/v] in air at 37°C) in an antibiotic solution (Dulbecco's modified Eagle's medium [DMEM; Invitrogen] containing amphotericin B [25 μg·mL^{-1}; Sigma], vancomycin [0.05 mg·mL^{-1}; Sigma], gentamicin [0.5 mg·mL^{-1}; Sigma], polymyxin B [0.2 mg·mL^{-1}; Autogen Bioclear Ltd.], primaxin [0.2 mg·mL^{-1}; VWR], and aprotinin [10 KIU·mL^{-1}]) for 8–16 h. Tissue was then cut into 1 mm^3 pieces and placed in digestion solution (0.1% [w/v] collagenase and 0.1% [w/v] hyaluronidase I-S; Sigma) overnight at 37°C with agitation. Once digested the debris was filtered through a 100 μm cell sieve. The cell suspension was then centrifuged (200 *g*, 10 min) and the supernatant discarded. The cell pellet was then resuspended in 5 mL of standard culture medium consisting of DMEM containing 10% (v/v) fetal calf serum (Biosera), 1 mM L-glutamine (Invitrogen), penicillin (100 U·mL^{-1}; Invitrogen), and streptomycin (100 μg·mL^{-1}; Invitrogen) before aliquoting into a 25 cm^3 flask. Cells were incubated until subconfluent at 37°C in 5% (v/v) CO_2 in air and passaged to allow expansion of cell numbers.

Phenotype of cultured cells

Meniscal cells were extracted from porcine medial menisci as described above. Primary human dermal fibroblasts

(PHDFs) were purchased from Cascade Biologics. The phenotype of the cells was determined using immunofluorescent labeling with the following monoclonal antibodies: porcine medial meniscal cells (PMMCs)—(1) collagen type I (Millipore), (2) collagen type II (Millipore), (3) collagen type VI (Millipore), (4) CD34 (Serotec), (5) vimentin (Vector Laboratories), (6) chondroitin sulfate (Sigma), (7) fibronectin (Vector Laboratories), (8) α-smooth muscle actin (Sigma), (9) desmin (Novocastra); PHDFs—(1) collagen type I, (2) fibronectin, (3) vimentin, and (4) Ki-67 (Dako). A goat anti-mouse secondary antibody conjugated to fluorescein (Alexa Fluor 488; Invitrogen) was used to observe the primary antibodies. Phenotype analysis was carried out at passage 1–4. Positive control tissue assessed the functionality of each antibody (porcine skin for collagen type I and fibronectin; porcine cartilage for the collagen types II, VI and chondroitin sulfate; porcine muscle for vimentin, α-smooth muscle actin and desmin; porcine bone marrow smear for CD34 and a proliferating cell line for Ki-67). Omission of the primary antibody and use of the appropriate isotype controls (IgG_1, IgG_{2a}, and IgM; Dako) served as the negative controls.

Attachment of porcine medial meniscal cells and human dermal fibroblasts to decellularized porcine medial meniscal tissue

The flattened, inferior surface of the meniscal tissue was found to be suitable for cell seeding. A 2–3-mm-thick layer was sheered off using a scalpel blade and a 1.5 cm^2 square section was then cut out from the central section. This tissue was placed between custom-made galvanized inner steel rings, which allowed definition of the area of tissue to be seeded (0.5 cm^2). Tightening of outer rings allowed a seal to be formed between the tissue and the inner rings.

The tissue/ring (seeding ring) constructs were then placed individually in the wells of six-well plates. The decellularized porcine medial meniscal tissue surface was then preconditioned with 0.5 mL of standard culture medium for 3 h at 37°C in an atmosphere of 5% (v/v) CO_2 in air. In addition, standard culture medium (2.5 mL) was added to the wells containing the seeding ring constructs.

In preparation for their use, cells were subcultured to ~60% confluency. Before their application, the preconditioning medium was removed from the acellular scaffolds and the following cell densities were prepared using DMEM as diluent: (1) PHDFs; 12×10^3, 12×10^4 and 12×10^5 cells/mL^{-1} and (2) PMMCs; 8×10^3, 8×10^4 and 8×10^5 cells/mL^{-1}. Each cell suspension (250 μL) was then applied to the decellularized meniscal samples ($n=3$). After 3 h of culture, the medium was aspirated and 250 μL of standard culture medium was added to each seeding ring. This was left to incubate at 37°C in an atmosphere of 5% (v/v) CO_2 in air for a further 21 h. The tissue was then removed, divided into two and one half processed for histology and one half processed for scanning electron microscopy (SEM) analysis to assess cell coverage and morphology.

Infiltration of porcine medial meniscal cells and human dermal fibroblasts into decellularized porcine medial meniscal tissue

To assess whether cells were able to infiltrate into the acellular porcine medial meniscal scaffold, an extended cell culture study was performed. This involved incubating the optimum cell concentration ([1] PHDFs; 12×10^5 cells/mL^{-1} and [2] PMMCs; 8×10^5 cells/mL^{-1}) on the decellularized porcine medial meniscal scaffold ($n=3$; dissected as above) for 7 days. The cells were seeded onto the acellular tissue as described above. The seeding rings were removed after the first 24 h, leaving the tissue in the medium of the six-well plate well. The medium was changed every 2 days. After 7 days of incubation at 37°C in an atmosphere of 5% (v/v) CO_2 in air, the samples were removed. Each sample was halved to allow SEM and histological analysis to be performed on all the samples to assess cell coverage, infiltration, and morphology.

Histological assessment of cell-seeded decellularized porcine medial meniscal tissue

Cell-seeded decellularized meniscal samples ($n=3$) were fixed in 10% (v/v) neutral buffered formalin for 48 h and then dehydrated using an automated process before embedding samples in paraffin wax. Serial sections of 6 μm in thickness were taken with 1 in 10 sections used. Standard H&E staining was used to evaluate tissue histoarchitecture. Deoxyribonucleic acid was stained using Hoechst dye (bisbenzimide H33258 pentahydrate; Molecular Probes). Images were captured digitally and assessed qualitatively.

SEM of cell-seeded acellular porcine medial meniscal tissue

Cell-seeded decellularized meniscal samples ($n=3$) were fixed with 2.5% (w/v) glutaraldehyde/PBS and postfixed with 1% (w/v) osmium tetroxide and then dehydrated using an ascending alcohol series. The samples were then critical point dried using a Polaron E3000 critical point drying apparatus (Aztech Trading) using liquid CO_2 as the transition fluid. Specimens were mounted using carbon cement and coated with gold using a Polaron E5300 freeze dryer sputter coating unit. Specimens were then observed and imaged using a CamScan 3-30BM scanning electron microscope (Aztech Trading) to evaluate the cell coverage and morphology.

Data analysis

All numerical data were analyzed using Microsoft Excel 2003. Means, standard deviations, and 95% confidence limits were calculated for each set of results. For comparison of groups of two means, the Student's *t*-test was used. Data with more than two groups were analyzed by one-way analysis of variance (ANOVA) followed by calculation of the minimum significant difference ($p<0.05$) using the T-method.

In cases where calculated data were expressed in percentage or proportions, data were transformed to arcsine (inverse sine) values to allow accurate generation of 95% confidence limits. After conversion, 95% confidence intervals were calculated using the arcsine values. Data were then transformed back to percentage/proportional values for presentation.

Results

In vivo *immunocompatibility study*

After 3 months implantation, all mice were humanly sacrificed using a UK Home Office–approved method. Tissues

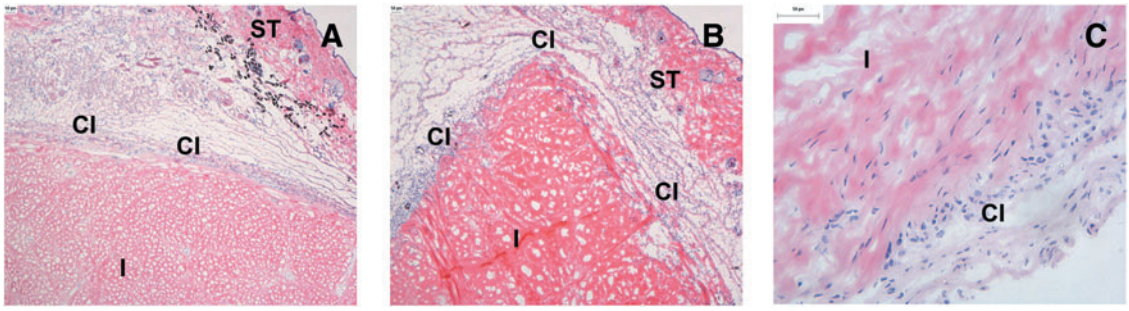

FIG. 2. Histological images of fresh/decellularized porcine medial meniscal tissue after 3-month subcutaneous implantation in GTKO mice vaccinated with porcine red blood cells. **(A)** H&E-stained fresh porcine medial meniscal tissue surrounded by fibrous capsule, 40× mag; **(B)** H&E-stained acellular porcine medial meniscal tissue surrounded by fibrous capsule, 40× mag; **(C)** H&E-stained acellular porcine medial meniscal tissue showing cellular infiltration, 200× mag. CI, capsular interface; GTKO, galactosyltransferase knock-out; H&E, hematoxylin and eosin; I, meniscal implant; mag, magnification; ST, murine subcutaneous mouse tissue. Color images available online at www.liebertonline.com/ten.

were explanted together with the surrounding mouse skin for analysis. However, not all of the implants were retrieved. Of the vaccinated group there were four of four recovered in the fresh, four of six in the decellularized, and three of four in the α-galactosidase-treated group. Of the nonvaccinated group there were four of four recovered in the fresh, four of six in the decellularized, and three of four in the α-galactosidase-treated group.

Macroscopic examination of explanted tissue. On gross observation, no areas of inflammation were observed on the mouse skin located over the explants. All explanted fresh, decellularized, and α-galactosidase-treated tissues from vaccinated/nonvaccinated mice were white and glossy. Tissues had maintained their native rigid-like constituency and there were no obvious signs of tissue shrinkage.

Microscopic examination of H&E-stained explants. The explanted tissue extracellular matrices from all the groups were in good condition with no obvious signs of matrix damage. Cells had readily infiltrated the entire periphery of the explants (Fig. 2). These cells had a varied morphology, with the majority of cells having a fibroblastic-like morphology aligned with the collagen orientation (Fig. 2C). Also present in small quantities were mononuclear cells. The centers of the explants were relatively acellular. A small number of cells were present within the center of some of the explants but this was not a consistent finding. All of the explants were surrounded by a fibrous capsule, which was populated with cells that were mainly of a mononuclear morphology.

Determination of thickness of the fibrous capsule surrounding explants. To measure the foreign body response to the implants, a series of measurements were taken to determine capsule thickness. The thickness of the capsule was significantly greater in the fresh tissue explant compared to the decellularized and α-galactosidase treated samples for both nonvaccinated and vaccinated mice (Fig. 3). For both nonvaccinated and vaccinated groups there was no significant

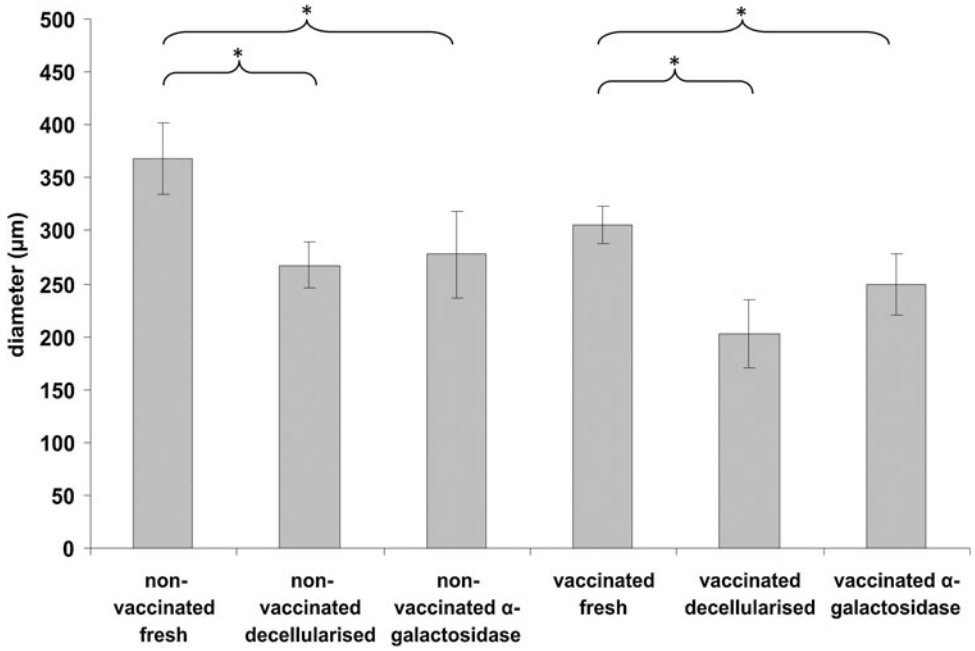

FIG. 3. Capsule thickness of fresh, decellularized, α-galactosidase-treated porcine medial meniscal explants from nonvaccinated/vaccinated GTKO mice. The error bars represent 95% confidence limits ($n = 3$). *A significant difference as determined by analysis of variance ($p < 0.05$).

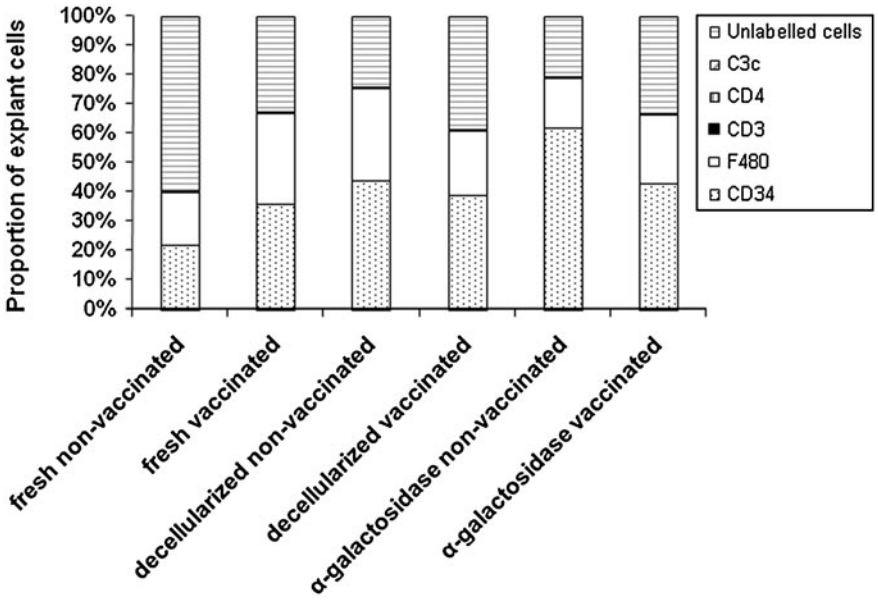

FIG. 4. Phenotype analysis of cellular infiltrate of fresh, decellularized, and α-galactosidase-treated porcine medial meniscal samples after 3-month implantation in nonvaccinated and vaccinated GTKO mice. Error bars have been removed for presentation purposes; however, data represent the mean ($n = 3$).

difference between the decellularized and the α-galactosidase-treated explants (Fig. 3).

Phenotype of cells infiltrating the tissue explants. Mouse spleen allowed verification of the functionality of antibody to CD3, CD4, CD34, and F4/80 (data not shown). Labeling was localized to the ECM in a banded pattern (data not shown). Mouse kidney allowed verification of the functionality of antibody to C3c with labeling diffusely located throughout the cortex (data not shown). Negative controls (isotype and primary antibody omission) verified antibody specificity with no positive labeling found (data not shown).

Nonvaccinated mice: Evaluation of porcine medial meniscal implants in nonvaccinated GTKO mice showed that for all three groups the majority of cells were located in the fibrous capsule. The cells were mainly F4/80 positive (mononuclear phagocytes) with occasional, rare CD3 and CD4-positive cells.

Within the explant tissue the majority of cells were F4/80 or CD34 positive in all of the explant groups (Fig. 4). There was no significant difference between the proportion of CD34 and F4/80-positive cells between the three groups, with the exception of the α-galactosidase-treated tissue, which had significantly more CD34-positive cells (Fig. 4). Extremely low numbers of cells positive for CD3 and CD4 were found in the explants (Fig. 4). No tissues were positive for C3c (Fig. 4). Unlabeled cells, negative for CD3, CD4, F4/80, and CD34, also accounted for a large proportion of the cells infiltrating the tissues (Fig. 4). These cells had a fibroblastic morphology. Comparison between the groups (fresh, decellularized, and α-galactosidase-treated samples) showed that the fresh tissue contained a significantly lower proportion of CD34-positive cells in comparison with the α-galactosidase-treated samples (ANOVA $p < 0.05$; Fig. 4). There was a lower proportion of F4/80-positive cells in the fresh explants compared to the decellularized samples (Fig. 4). There was a significantly higher proportion of unlabelled cells in the fresh samples on compared to both the decellularized and α-galactosidase-treated samples (ANOVA $p < 0.05$; Fig. 4).

Vaccinated mice: The cells of the capsule were predominantly made up of F4/80-positive cells and low numbers of CD3 and CD4-positive cells (Fig. 4).

Analysis of the cells infiltrating the explants revealed that there was no significant differences in the proportion of CD34, F4/80, and unlabeled cells between the three groups. Extremely low numbers of cells were positive for CD3 and CD4. No explants were positive for C3c (Fig. 4).

Determination of anti-α-gal antibodies in GTKO mouse serum. The mean titer of anti α-gal antibodies was determined for each mouse group. The titers were converted to antibody units by taking the reciprocal of the titer. Vaccinated mice that were implanted with fresh, decellularized, and α-galactosidase meniscal tissue recorded 240, 480, and 1260 antibody units, respectively. Nonvaccinated mice that were implanted with fresh, decellularized, and α-galactosidase meniscal tissues recorded 10, 80, and 25 antibody units, respectively. Data were then pooled into vaccinated and nonvaccinated subgroups. Nonvaccinated mice achieved a mean of 44 antibody units, whereas vaccinated mice had a mean of 463 antibody units.

Phenotypic characterization of cultured cells

Meniscal cells were found to be positive for collagen I, II, CD34, chondroitin sulfate, desmin, vimentin, fibronectin, and α-smooth muscle actin. However, staining for collagen VI was not present (data not shown). A smaller panel was used to identify human dermal fibroblasts as being positive for collagen type I, fibronectin, vimentin, and Ki-67 (data not shown). Positive control tissues and negative controls (isotype and primary antibody omission) confirmed functionality and specificity of primary antibodies (data not shown).

Histological and SEM assessment of attachment of PHDFs and porcine medial meniscal cells to the acellular porcine meniscal scaffold

The approximate confluent cell density (CCD) in monolayer culture of each cell type was established and found to

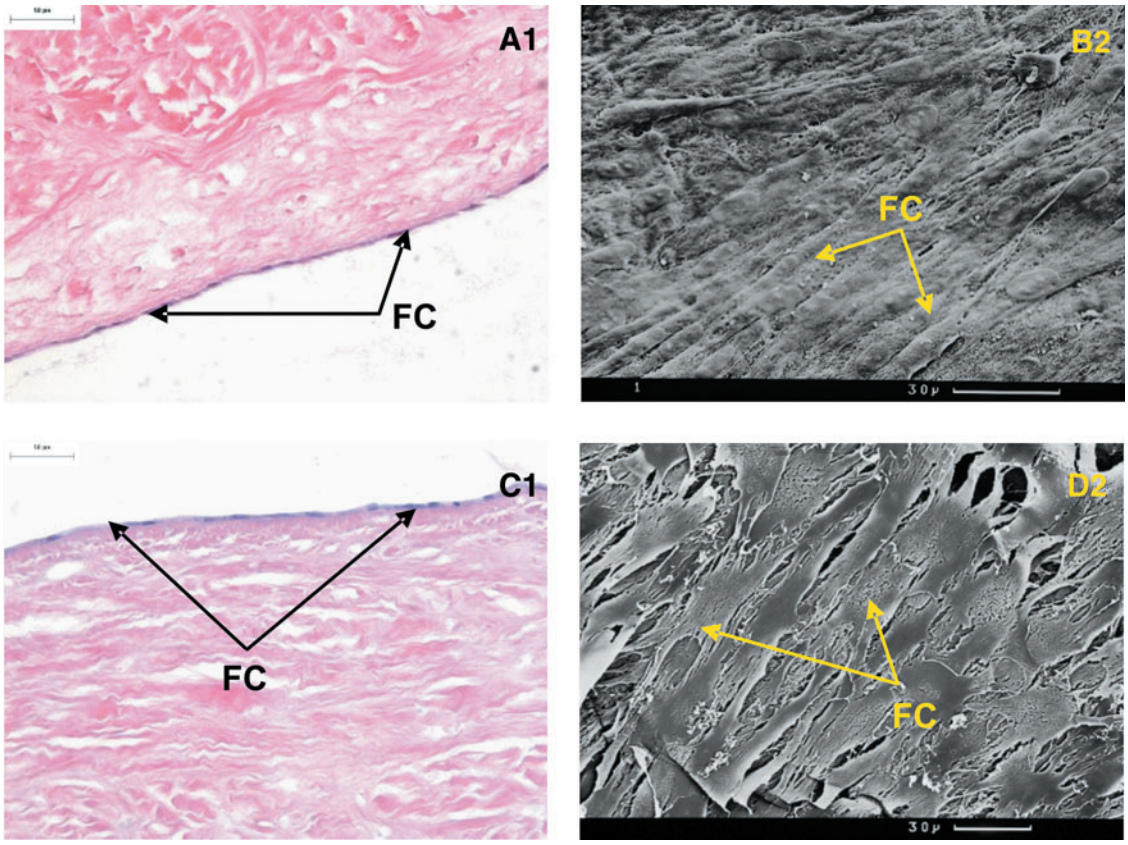

FIG. 5. Histology and SEM of acellular porcine medial meniscal tissue after 24 h culture with **(A1, B2)** human dermal fibroblasts and **(C1, D2)** porcine medial meniscal cells at 37°C in an atmosphere of 5% (v/v) CO_2 in air. Cells were seeded at the following concentrations: **(A1, B2)** 6×10^5 cells/cm^2 and **(C1, D2)** 4×10^5 cells/cm^2. Analysis were performed using (1) H&E staining, 200× mag and (2) SEM. Scale bar represents 30 μm. FC, flattened cells; SEM, scanning electron microscopy. Color images available online at www.liebertonline.com/ten.

be 4×10^3 cells/cm^2 for PHDFs and 6×10^3 cells/cm^2 for PMMCs. Each cell type was then seeded onto samples of the acellular scaffold at the established CCD and 10-fold and 100-fold above this density.

For PHDFs, seeding at the CCD resulted in a limited degree of cellular attachment. SEM analysis of the attached cells showed that not all the attached cells were flattened and many appeared raised from the tissue surface. At a seeding density 10-fold above CCD cellular attachment was improved and the cells took on a flattened appearance. At a seeding density 100-fold above CCD optimal attachment was observed; the cells formed a complete monolayer across the tissue surface with tightly packed cells aligning in the same direction (Fig. 5A1). This was confirmed by SEM analysis showing aligned flattened cells across the surface of the tissue (Fig. 5B2). For all the samples, no cell infiltration into the acellular scaffold was found after 24 h incubation.

For PMMCs a similar result was obtained with cell attachment improving with increasing seeding density. Samples seeded at the CCD revealed cellular attachment with the majority of cells exhibiting a flattened appearance; however, a few rounded cells were also present. Increasing the seeding density by 10-fold resulted in further cell attachment. Cells again took on a flattened appearance and were in contact with one another. The seeding density 100-fold above CCD resulted in the highest degree of cellular attachment, with a monolayer-like coverage of the acellular porcine medial meniscal scaffold (Fig. 5C1). SEM analysis showed the cells to be of a flattened morphology and very tightly packed (Fig. 5D2). No infiltration into the acellular scaffold was found after 24 h incubation.

Histological and SEM assessment of infiltration of PHDFs and porcine medial meniscal cells into the acellular porcine meniscal scaffold

Acellular porcine medial meniscal tissue was cultured for 7 days with the cells at 100× CCD. PHDFs formed a stacked layer of cells (Fig. 6A, B). Two of the three samples showed cellular infiltration upon histological analysis (~150 μm in depth) with up to eight cells per field of view at 100× magnification (Fig. 6C). Hoechst staining confirmed the presence of DNA within these cell-like structures (Fig. 6D). SEM analysis confirmed that the cells on the surface appeared flattened and aligned in a similar direction to one another (Fig. 6E, F).

With regard to PMMCs, cell attachment was maintained after 7 day culture. H&E and Hoechst staining revealed the retention of a monolayer-like structure across the surface of the acellular porcine medial meniscal scaffold (Fig. 7A, B). SEM analysis showed that the cells were morphologically flattened, circular, and in contact with one another. In addition, gaps were found interspersed between various cell

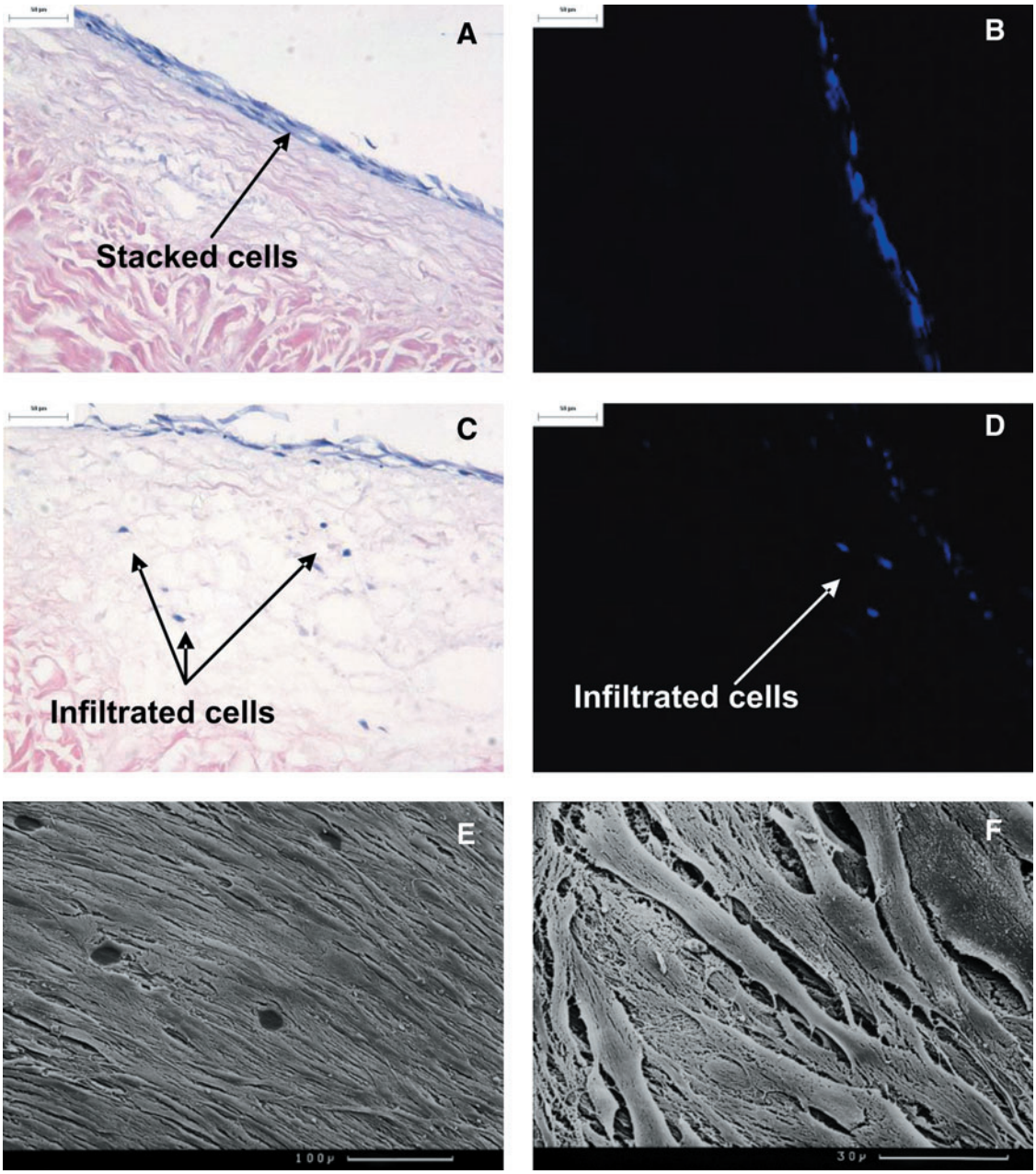

FIG. 6. Histology and SEM of acellular porcine medial meniscal tissue after 7-day culture with primary human dermal fibroblasts at 37°C (continues overleaf) in an atmosphere of 5% (v/v) CO_2 in air. Cells were seeded at 6×10^5 cells/cm^2. **(A)** Image of stacked cells on the acellular scaffold, stained with H&E, 200× mag; **(B)** image of stacked cells on the acellular scaffold, stained with Hoechst 33258 dye, 200× mag; **(C)** image of cells infiltrated into the acellular scaffold, stained H&E, 200× mag; **(D)** image of cells infiltrated into the acellular scaffold, stained with Hoechst 33258 dye, 200× mag; **(E)** SEM image of cell monolayer viewed from above, scale bar represents 100 μm; **(F)** SEM image of cell monolayer viewed from above, scale bar represents 30 μm. Color images available online at www.liebertonline.com/ten.

patches of the monolayer (Fig. 7C, D). There was no evidence of cellular infiltration into the acellular scaffold.

Discussion

There is an increasing need for meniscal replacement driven by a greater incidence of knee injuries in which the meniscus is damaged irreparably. The reasons for this have been attributed to the higher proportion of people participating in sports such as skiing that place extreme stresses on the knee.[20]

Currently, the best treatment is replacement with an allograft; however, allografts have been associated with problems of disease transmission and immune rejection.[6,7,21–24] Other options include meniscal replacements such as the CMI™ (commercially known as Menaflex™) that utilize reconstituted swollen bovine collagen that acts as a natural prosthesis to allow cellular ingrowth. U.S. Food and Drug Administration approval has recently been granted for its use after partial meniscectomy; however, its use is limited to patients with intact meniscal rims. Clinical findings

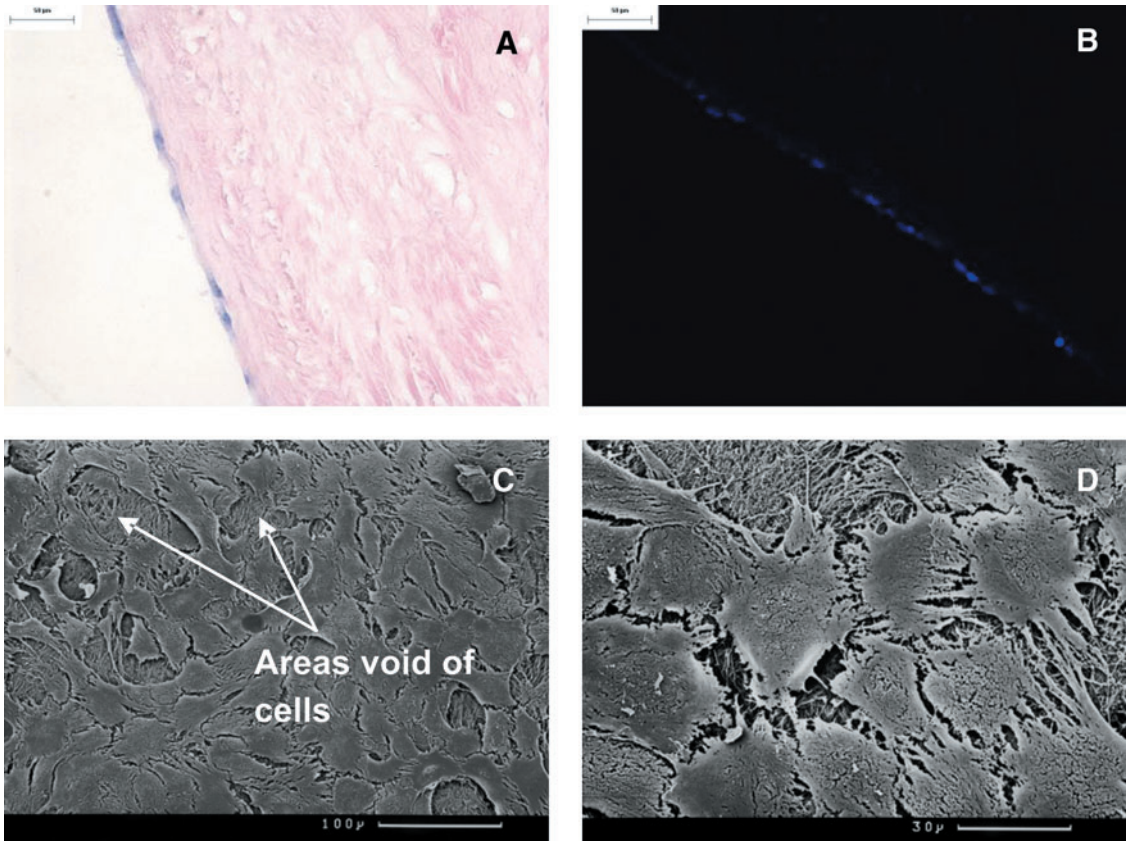

FIG. 7. Histology and SEM of acellular porcine medial meniscal tissue after 7 day culture with primary porcine meniscal cells at 37°C in an atmosphere of 5% (v/v) CO_2 in air. Cells were seeded at 4×10^5 cells/cm^2. **(A)** Image of cellular monolayer on the acellular scaffold, stained with H&E, 200× mag; **(B)** image of cellular monolayer on the acellular scaffold, stained with Hoechst 33258 dye, 200× mag; **(C)** SEM image of cell monolayer viewed from above, scale bar represents 100 μm; **(D)** SEM image of cell monolayer viewed from above, scale bar represents 30 μm. Color images available online at www.liebertonline.com/ten.

have been inconclusive with regard to chondroprotection.[25–29]

A key choice in the development of a tissue-engineered implant is whether to engineer a cellularized construct.[29–36] Cellularized scaffolds may be particularly important when the cells are necessary for maintenance of the surrounding matrix or have an important function, for example, preservation of the antithrombogenicity of a vascular conduit via endothelization or simply to aid continual growth in young recipients.[30,31] Acellular scaffolds have the advantage of delivery as medical devices and avoid the regulatory issues associated with the delivery of living constructs, which require long-term culture in bioreactors. Acellular scaffolds rely upon *in vivo* regeneration by endogenous cells, with the living host acting as a bioreactor. This latter approach has enabled an acellular meniscal scaffold to progress to clinical translation,[29] whereas cellularized constructs have not yet progressed from the experimental or preclinical stage.[16,37] This study aimed to assess the immunocompatibility and cellularization potential of an acellular porcine medial meniscal scaffold.

Previous studies established the removal of the immunogenic carbohydrate, α-gal epitope after decellularization of porcine medial menisci.[14] In addition, it was shown that the acellular porcine medial meniscus was not cytotoxic *in vitro.* This satisfied the ethical criteria for implantation into mice to determine *in vivo* immunocompatibility. The GTKO mouse model was selected to represent the immunological status of human with regard to the α-gal epitope. The GTKO mouse lacks the α-galactosyl transferase gene but is immunologically normal. The inflammatory/immune response to native and acellular tissues was evaluated in GTKO mice that had or had not been immunized with porcine red blood cells to increase antibody titers to the α-gal epitope. Three groups of tissues were implanted subcutaneously: fresh, acellular, and acellular tissue treated with α-galactosidase to remove any residual α-gal and act as a control. A limitation of this study was that the wounds were not sutured since, in our previous experience, sutures can evoke an inflammatory response with T-cell infiltration and calcification. Blunt dissection under the skin allowed placement distant from the incision; however, 6 of the total 28 implants were lost reducing the power of the study; notwithstanding this, there were a total of 8 fresh, 8 decellularized, and 6 α-galactosidase-treated decellularized explants recovered for analysis from immunized and nonimmunized mice.

Upon explantation, all of the tissues were surrounded by a loosely bound capsule comprised of mononuclear phagocytes with cells infiltrating the periphery of the tissues after the collagen orientation. Capsule thickness provided a simple method of quantifying the response and this showed a thicker capsule surrounding the fresh tissue explants for both

vaccinated and nonvaccinated mice. To determine any differences between the nature and quantity of the infiltrating cells, direct counting of cells stained by immunohistochemistry using antibodies to F4/80 (mononuclear phagocytes), CD34 (endothelial progenitor cells), CD3 (pan T-cell), and CD4 (helper T-cells) was performed. Weaknesses of this approach were that a large proportion of the infiltrating cells, of fibroblastic morphology, were not characterized using the antibody panel and only thin sections of the explanted tissues were analyzed. Hence, a full numerical analysis of the cellular infiltrates present within the full thickness of the tissues was not carried out. Alternative methods such as the use of the stereological optical dissector principle or isolation of the cells and characterization by flow cytometry would not have been appropriate due to the dense nature of the meniscal tissue and sparse numbers of infiltrating cells.

The cellular infiltrate into all the tissues comprised mononuclear phagocytes, CD34-positive cells, and unlabelled fibroblastic cells. It is of particular note that CD3 and CD4-positive cells were virtually nonexistent, indicating a lack of specific immune response to any of the implants, including the fresh meniscal tissue. There was also an absence of C3c deposition (indicative of immune complexes), in both the vaccinated and nonvaccinated mice, despite a 12-fold elevation of antibodies to α-gal in the vaccinated group. The lack of immune reaction to the fresh meniscal tissue may have been associated with the dense extracellular matrix combined with the relatively sparse cell and α-gal epitope density characteristic of this tissue. Indeed, the limited antigenicity and immunoprivileged qualities of meniscal tissue has been previously reported.[38,39] However, longer term studies are required to support this claim. The lack of a positive response to the fresh meniscal tissue questions the validity of the model. However, parallel studies in the same laboratory showed that fresh porcine ureter elicited a predictable immune response comprising CD3-positive cells and macrophages in GTKO mice.[40] In addition, the fresh porcine ureter tissue explants exhibited a vacuolated appearance consistent with necrosis. These previously reported results validated the model, despite the lack of a significant immune response to the fresh meniscal tissue in this study. These studies also highlight the differences between the dense meniscal extracellular matrix and that of the ureter.

The specific aim of this *in vivo* study was to determine the immunocompatibility of the acellular porcine meniscus, and this aim was met. It could be concluded that decellularization of porcine meniscal tissue is not necessary for immune acceptance. However, decellularization offers considerable advantages, including clinical translation as a medical device due to the absence of functional DNA, with a much more straight forward regulatory pathway compared to a cellular xenograft.

The presence of mononuclear phagocytes in the periphery of the tissues with endothelial progenitors and fibroblast-like cells in the acellular scaffolds could indicate a regenerative/wound healing type response, or a nonspecific inflammatory response. However, the lack of overt tissue damage, relatively sparse capsule surrounding the acellular scaffolds, and presence of fibroblast-like cells and endothelial progenitors in the depth of the tissue favor the former. Previous studies of acellular porcine extracellular matrix in rats have identified macrophages predominantly of the M2 phenotype (CD163 positive) associated with tissue remodeling rather than the M1 subset (CCR7 positive) involved in inflammation.[41–43] Extensive attempts to classify the mononuclear phagocytes in the explants using similar murine markers proved unsuccessful. Longer term temporal studies together with molecular analysis of gene expression are required to resolve this issue.

PHDFs and PMMCs were used to assess whether cells could attach to and infiltrate the acellular porcine medial meniscal scaffold *in vitro*. The strategy was to evaluate native porcine medial meniscal cells (PMMCs) and human cells (PHDFs) that could be readily obtained from a patient. Porcine meniscal cells were positive for collagen type I, collagen type II, CD34, vimentin, chondroitin sulfate, fibronectin, α-smooth muscle actin, and desmin, but not for collagen VI. This indicated a mixed cell phenotype as reported previously.[44–53] However, it was not deemed necessary to purify a specific cell type for the purposes of this study. With regard to human dermal fibroblasts they were positive for collagen type I, fibronectin, vimentin, and Ki-67, indicating that the cells were in a proliferative state.

Both primary PMMCs and PHDFs attached to the acellular porcine meniscal tissue, verifying the potential of porcine tissue, decellularized with sodium dodecyl sulfate, to support cell survival.[14,54–56] After establishment of the optimum seeding density, culture was extended up to 7 days. This allowed preliminary investigations into whether the cells would migrate into the acellular porcine meniscal tissue *in vitro*. PMMCs remained attached and exhibited a flattened morphology. In addition, the cells spread out from one another, leaving gaps visible by SEM analysis, indicating that these cells might prefer a limited amount of cell contact as seen *in situ*. PHDFs differed in their response, with cells stacking to form between two and four layers of cells. Histological analysis confirmed that the cells were able to infiltrate into the acellular scaffolds up to a depth of $\sim 150\,\mu m$ in the 7-day period. Overall, the data supported the hypothesis that the acellular porcine meniscus provides a scaffold conducive to cellular attachment with evidence of potential for cellular infiltration both *in vitro* and *in vivo*.

The question arises whether it would be beneficial to pursue *in vitro* recellularization before implantation. It is likely that replacing the meniscus with a cellularized construct would result in loss of the viable donor cells after transplantation. It could be hypothesized that the presence of cells upon implantation would be detrimental since the structure is unlikely to become rapidly vascularized, leading to donor cell death with potential damage to the surrounding matrix. Indeed, it has been shown that when meniscal allografts are transplanted, host cells repopulate the meniscus with no evidence of donor cells remaining.[57] In the case of meniscal replacement, it is our opinion that an acellular meniscal scaffold will result in favorable remodeling upon clinical implantation.[58] Indeed, the decellularization methods applied in this study could also be applied to human donor tissue.

In conclusion, acellular porcine meniscal tissue exhibits excellent immunocompatibility and potential for cellular regeneration in the longer term.

Future work will test the porcine meniscal scaffold in a functional large animal model (ovine) of meniscal repair. This will establish the *in vivo* regenerative capacity of the acellular meniscal scaffold over the longer term.

Acknowledgments

Funding support was from (1) Engineering and Physical Science Research Council. Portfolio Partnership: Tissue Replacement and Regeneration (GR/S63892/01). (2) EPSRC DTA studentship to Thomas W. Stapleton; (3) National Institute for Health Research (NIHR) as part of a collaboration with the Leeds Musculoskeletal Biomedical Research Unit. John Fisher is an NIHR senior investigator.

Disclosure Statement

Professor E. Ingham and Professor J. Fisher are directors of Tissue Regenix, Ltd., to which the decellularization technology is licensed.

References

1. Rath, E., and Richmond, J.C. The menisci: basic science and advances in treatment. Br J Sports Med **34,** 252, 2000.
2. Boyd, K.T., and Myers, P.T. Meniscus preservation; rationale, repair techniques and results. Knee **10,** 1, 2003.
3. Baratz, M.E., Fu, F.H., and Mengato, R. Meniscal tears: the effect of meniscectomy and of repair on intraarticular contact areas and stress in the human knee. A preliminary report. Am J Sports Med **14,** 270, 1986.
4. Burke, D.L., Ahmed, A.H., and Miller, J. A biomechanical study of partial and total medial meniscectomy of the knee. Trans Orthop Res Soc **3,** 91, 1978.
5. Altman, G.H., Horan, R.L., Lu, H.H., Moreau, J., Martin, I., Richmond, J.C., and Kaplan, D.L. Silk matrix for tissue engineered anterior cruciate ligaments. Biomaterials **23,** 4131, 2002.
6. Patel, R., and Trampuz, A. Infections transmitted through musculoskeletal-tissue allografts. N Engl J Med **350,** 2544, 2004.
7. Tomford, W.W. Transmission of disease through transplantation of musculoskeletal allografts. J Bone Joint Surg Am **77,** 1742, 1995.
8. Welsing, R.T.C., van Tienen, T.G., Ramrattan, N., Heijkants, R., Schouten, A.J., Veth, R.P.H., and Buma, P. Effect on tissue differentiation and articular cartilage degradation of a polymer meniscus implant. Am J Sports Med **36,** 1978, 2008.
9. Cook, J.L., and Fox, D.B. *In vitro* and *in vivo* evaluation of synthetic conduits for augmentation of avascular meniscal healing and regeneration. Abstract presented at the Orthopaedic Research Society, Chicago, IL, 2006. Abstract no. 1032.
10. Stone, K.R., Steadman, J.R., Rodkey, W.G., and Li, S.T. Regeneration of meniscal cartilage with use of a collagen scaffold. Analysis of preliminary data. J Bone Joint Surg Am **79,** 1770, 1997.
11. Maier, D., Braeun, K., Steinhauser, E., Ueblacker, P., Oberst, M., Kreuz, P.C., Roos, N., Martinek, V., and Imhoff, A.B. *In vitro* analysis of an allogenic scaffold for tissue-engineered meniscus replacement. J Orthop Res **25,** 1598, 2007.
12. Aufderheide, A.C., and Athanasiou, K.A. Assessment of a bovine co-culture, scaffold-free method for growing meniscus-shaped constructs. Tissue Eng **13,** 1, 2007.
13. Peretti, G.M., Gill, T.J., Xu, J.W., Randolph, M.A., Morse, K.R., and Zaleske, D.J. Cell-based therapy for meniscal repair: a large animal study. Am J Sports Med **32,** 146, 2004.
14. Stapleton, T.W., Ingram, J., Katta, J., Knight, R., Korossis, S., Fisher, J., and Ingham, E. Development and characterization of an acellular porcine medial meniscus for use in tissue engineering. Tissue Eng Part A **14,** 505, 2008.
15. Steadman, J.R., and Rodkey, W.G. Tissue-engineered collagen meniscus implants: 5- to 6-year feasibility study results. Arthroscopy **21,** 515, 2005.
16. Yamasaki, T., Deie, M., Shinomiya, R., Izuta, Y., Yasunaga, Y., Yanada, S., Sharman, P., and Ochi, M. Meniscal regeneration using tissue engineering with a scaffold derived from a rat meniscus and mesenchymal stromal cells derived from rat bone marrow. J Biomed Mater Res A **75,** 23, 2005.
17. Tan, Y., Zhang, Y., and Pei, M. Meniscus reconstruction through co-culturing meniscus cells with synovium-derived stem cells on small intestine submucosa—a pilot study to engineer meniscus tissue constructs. Tissue Eng Part A **16,** 67, 2010.
18. Verdonk, R. Alternative treatments for meniscal injury. J Bone Joint Surg Br **79,** 866, 1997.
19. Lomas, R.J., Cruse-Sawyer, J.E., Simpson, C., Ingham, E., Bojar, R., and Kearney, J.N. Assessment of the biological properties of human split skin allografts disinfected with peracetic acid and preserved in glycerol. Burns **29,** 515, 2003.
20. Majewski, M., Susanne, H., and Klaus, S. Epidemiology of athletic knee injuries: a 10-year study. Knee **13,** 184, 2006.
21. Nemzek, J.A., Arnoczky, S.P., and Swenson, C.L. Retroviral transmission by the transplantation of connective-tissue allografts. An experimental study. J Bone Joint Surg Am **76,** 1036, 1994.
22. Prokopis, P.M., and Schepsis, A.A. Allograft use in ACL reconstruction. Knee **6,** 75, 1999.
23. Rodeo, S.A., Seneviratne, A., Suzuki, K., Felker, K., Wickiewicz, T.L., and Warren, R.F. Histological analysis of human meniscal allografts. A preliminary report. J Bone Joint Surg Am **82,** 1071, 2000.
24. Golshayan, D., Buhler, L., Lechler, R.I., and Pascual, M. From current immunosuppressive strategies to clinical tolerance of allografts. Transpl Int **20,** 12, 2007.
25. Reguzzoni, M., Manelli, A., Ronga, M., Raspanti, M., and Grassi, F.A. Histology and ultrastructure of a tissue-engineered collagen meniscus before and after implantation. J Biomed Mater Res B Appl Biomater **74,** 808, 2005.
26. Buma, P., van Tienen, T., and Veth, R.P. The collagen meniscus implant. Expert Rev Med Devices **4,** 507, 2007.
27. Zaffagnini, S., Giordano, G., Vascellari, A., Bruni, D., Neri, M., Iacono, F., Kon, E., Presti, M., and Marcacci, M. Arthroscopic collagen meniscus implant results at 6 to 8 years follow up. Knee Surg Sports Traumatol Arthrosc **15,** 175, 2007.
28. Linke, R.D., Ulmer, M., and Imhoff, A.B. Replacement of the meniscus with a collagen implant (CMI). Oper Orthop Traumatol **18,** 453, 2006.
29. Rodkey, W.G., DeHaven, K.E., Montgomery, W.H., Baker, C.L., Jr., Beck, C.L., Jr., Hormel, S.E., Steadman, J.R., Cole, B.J., and Briggs, K.K. Comparison of the collagen meniscus implant with partial meniscectomy. A prospective randomized trial. J Bone Joint Surg Am **90,** 1413, 2008.
30. Hoerstrup, S.P., Cummings, I., Lachat, M., Schoen, F.J., Jenni, R., Leschka, S., Neuenschwander, S., Schmidt, D., Mol, A., Günter, C., Gössi, M., Genoni, M., and Zund, G. Functional growth in tissue-engineered living, vascular grafts: follow-up at 100 weeks in a large animal model. Circulation **114 Suppl,** I-159, 2006.
31. Hoerstrup, S.P., Sodian, R., Daebritz, S., Wang, J., Bacha, E.A., Martin, D.P., Moran, A.M., Guleserian, K.J., Sperling, J.S., Kaushal, S., Vacanti, J.P., Schoen, F.J., and Mayer, J.E., Jr.

Functional living trileaflet heart valves grown *in vitro*. Circulation **102,** III-44, 2000.
32. Egaña, J.T., Danner, S., Kremer, M., Rapoport, D.H., Lohmeyer, J.A., Dye, J.F., Hopfner, U., Lavandero, S., Kruse, C., and Machens, H.G. The use of glandular-derived stem cells to improve vascularization in scaffold-mediated dermal regeneration. Biomaterials **30,** 5918, 2009.
33. Cook, J.L., Fox, D.B., Malaviya, P., Tomlinson, J.L., Kuroki, K., Cook, C.R., and Kladakis, S. Long-term outcome for large meniscal defects treated with small intestinal submucosa in a dog model. Am J Sports Med **34,** 32, 2006.
34. Torikai, K., Ichikawa, H., Hirakawa, K., Matsumiya, G., Kuratani, T., Iwai, S., Saito, A., Kawaguchi, N., Matsuura, N., and Sawa, Y. A self-renewing, tissue-engineered vascular graft for arterial reconstruction. Thorac Cardiovasc Surg **136,** 37, 2008.
35. Saray, A. Porcine dermal collagen (Permacol) for facial contour augmentation: preliminary report. Aesthetic Plast Surg **27,** 368, 2003.
36. Yoshii, S., Ito, S., Shima, M., Taniguchi, A., and Akagi, M. Functional restoration of rabbit spinal cord using collagen-filament scaffold. J Tissue Eng Regen Med **3,** 19, 2009.
37. Yamasaki, T., Masataka, D., Shinomiya, R., Izuta, Y., Yasunaga, Y., and Ochi, M. Meniscal regeneration using mesenchymal stromal cells with a scaffold derived from a normal meniscus ~ efficacy of *ex vivo* meniscal transplantation in rats. Abstract presented at the Orthopaedic Research Society, Washington, DC, 2005. Abstract no. 1063.
38. Arnoczky, S.P., and Milachowski, K.A. Meniscal allograft: where do we stand? In: Ewing, W.J., ed. Articular Cartilage and Knee Joint Function: Basic Science and Arthroscopy. New York: Raven Press, 1990, pp. 129–136.
39. Garrett, J.C., Steensen, R.N., and Stevensen, R.N. Meniscal transplantation in the human knee: a preliminary report. Arthroscopy **7,** 57, 1991.
40. Derham, C., Yow, H., Ingram, J., Fisher, J., Ingham, E., Korrosis, S.A., and Homer-Vanniasinkam, S. Tissue engineering small-diameter vascular grafts: preparation of a biocompatible porcine ureteric scaffold. Tissue Eng Part A **14,** 1871, 2008.
41. Mantovani, A., Sica, A., and Locati, M. Macrophage polarization comes of age. Immunity **23,** 344, 2005.
42. Mills, C.D., Kincaid, K., Alt, J.M., Heilman, M.J., and Hill, A.M. M-1/M-2 macrophages and the Th1/Th2 paradigm. J Immunol **164,** 6166, 2000.
43. Brown, B.N., Valentin, J.E., Stewart-Akers, A.M., McCabe, G.P., and Badylak, S.F. Macrophage phenotype and remodeling outcomes in response to biologic scaffolds with and without a cellular component. Biomaterials **30,** 1482, 2009.
44. Hashimoto, J., Kurosaka, M., Yoshiya, S., and Hirohata, K. Meniscal repair using fibrin sealant and endothelial cell growth factor. An experimental study in dogs. Am J Sports Med **20,** 537, 1992.
45. Collier, S., and Ghosh, P. Effects of transforming growth factor beta on proteoglycan synthesis by cell and explant cultures derived from the knee joint meniscus. Osteoarthritis Cartilage **3,** 127, 1995.
46. Nabeshima, Y., Kurosaka, M., Yoshiya, S., and Mizuno, K. Effect of fibrin glue and endothelial cell growth factor on the early healing response of the transplanted allogenic meniscus: a pilot study. Knee Surg Sports Traumatol Arthrosc **3,** 34, 1995.
47. Spindler, K.P., Mayes, C.E., Miller, R.R., Imro, A.K., and Davidson, J.M. Regional mitogenic response of the meniscus to platelet-derived growth factor (PDGF-AB). J Orthop Res **13,** 201, 1995.
48. Wildey, G.M., and McDevitt, C.A. Matrix protein mRNA levels in canine meniscus cells *in vitro*. Arch Biochem Biophys **353,** 10, 1998.
49. Bhargava, M.M., Attia, E.T., Murrell, G.A., Dolan, M.M., Warren, R.F., and Hannafin, J.A. The effect of cytokines on the proliferation and migration of bovine meniscal cells. Am J Sports Med **27,** 636, 1999.
50. Tanaka, T., Fujii, K., and Kumagae, Y. Comparison of biochemical characteristics of cultured fibrochondrocytes isolated from the inner and outer regions of human meniscus. Knee Surg Sports Traumatol Arthrosc **7,** 75, 1999.
51. Nakata, K., Shino, K., Hamada, M., Mae, T., Miyama, T., Shinjo, H., Horibe, S., Tada, K., Ochi, T., and Yoshikawa, H. Human meniscus cell: characterization of the primary culture and use for tissue engineering. Clin Orthop Relat Res **391,** S208, 2001.
52. Zaleskas, J.M., Kinner, B., Freyman, T.M., Yannas, I.V., Gibson, L.J., and Spector, M. Growth factor regulation of smooth muscle actin expression and contraction of human articular chondrocytes and meniscal cells in a collagen-GAG matrix. Exp Cell Res **270,** 21, 2001.
53. Verdonk, P.C., Forsyth, R.G., Wang, J., Almqvist, K.F., Verdonk, R., Veys, E.M., and Verbruggen, G. Characterisation of human knee meniscus cell phenotype. Osteoarthritis Cartilage **13,** 548, 2005.
54. Ingram, J.H., Korossis, S., Howling, G., Fisher, J., and Ingham, E. The use of ultrasonication to aid recellularization of acellular natural tissue scaffolds for use in anterior cruciate ligament reconstruction. Tissue Eng **13,** 1561, 2007.
55. Wilcox, H.E., Korossis, S.A., Booth, C., Watterson, K.G., Kearney, J.N., Fisher, J., and Ingham, E. Biocompatibilty and recellularization potential of an acellular porcine heart valve. J Heart Valve Dis **14,** 228, 2005.
56. Gratzer, P.F., Harrison, R.D., and Woods, T. Matrix alteration and not residual sodium dodecyl sulfate cytotoxicity affects the cellular repopulation of a decellularized matrix. Tissue Eng **12,** 2975, 2006.
57. Jackson, D.W., Whelan, J., and Simon, T.M. Cell survival after transplantation of fresh meniscal allografts. DNA probe analysis in a goat model. Am J Sports Med **21,** 540, 1993.
58. Badylak, S.F. Regenerative medicine and developmental biology: the role of the extracellular matrix. Anat Rec B New Anat **287,** 36, 2005.

Address correspondence to:
Thomas W. Stapleton, Ph.D.
Institute of Molecular and Cellular Biology
The University of Leeds
Leeds, LS2 9JT
United Kingdom

E-mail: t.w.stapleton01@leeds.ac.uk

Received: December 16, 2009
Accepted: August 5, 2010
Online Publication Date: September 21, 2010